minated by $[Y_S]$ yields

$$[\alpha][V_{ii}(0)]1] = ([Y_S] + [Y][\alpha][\gamma]^{-1}[\alpha]^{-1})^{-1}I_S]. \quad (9a)$$

Here the apparent characteristic impedance is readily identified and agrees with Amemiya's result [3], [4]. The occurrence of the inverse modal matrix, however, would suggest difficulties with a system that is partially degenerate. This, of course, is the reason for the distinctness assumption. It is also the reason for the particular form of the modal matrix formation of (5). To clarify this, the fully degenerate case may be considered. If, for this case, $[V_{ii}]$ is interpreted as the voltage of line i to ground, i.e., if the word "modal" is ignored, and if $[\alpha]=[1]$, then (9a) becomes

$$V_{ii}(0)] = ([Y_S] + [Y][\gamma]^{-1})^{-1}I_S] \quad (9b)$$

which is exactly the fully degenerate solution. This would suggest that the modal matrix for the partially degenerate system may be constructed by partitioning. Thus if the first m eigenvalues are distinct and $s=n-m$ eigenvalues are equal, then $[\alpha]$ becomes

$$[\alpha] = \left[\begin{array}{c|c} \alpha(n,m) & \begin{array}{c} 0 \\ \hline 1(s,s) \end{array} \end{array}\right]. \quad (10)$$

Here the quantities in the parentheses denote the number of rows and columns of the submatrices. This form of $[\alpha]$ may be shown to be correct by rigorous calculations. It is convenient because it is nonsingular and because degeneracy may be introduced very simply by setting selected elements of α to zero. The earlier assumption of nondegeneracy is thus removed.

The reflection coefficients at the receiving end are due to the termination $[Y_R]$ at $x=L$. A straightforward evaluation yields

$$[V_{RR}]1] = [\epsilon^{-\gamma L}]([Y][\alpha][\gamma]^{-1} + [Y_R][\alpha])^{-1}([Y][\alpha][\gamma]^{-1} - [Y_R][\alpha])[\epsilon^{-\gamma L}][V_{ii}]1]. \quad (11)$$

The reflection coefficient at the receiving end is, therefore,

$$[\rho_R] = [\alpha]^{-1}[[Y_0] + [Y_R]]^{-1}[[Y_0] - [Y_R]][\alpha] \quad (12)$$

where

$$[Y_0] = [Y][\alpha][\gamma]^{-1}[\alpha]^{-1}.$$

The reflection coefficient at the sending end, $x=0$, may be obtained by subscript exchange. The unknown amplitudes become

$$\left.\frac{V_{kk}}{V_i}\right] = [\alpha][[\epsilon^{-\gamma x}] + [\epsilon^{-\gamma(L-x)}][\rho_R][\epsilon^{-\gamma L}]][[1] - [\rho_S][\epsilon^{-\gamma L}][\rho_R][\epsilon^{-\gamma L}]]^{-1}[\alpha]^{-1}([Y_S] + [Y_0])^{-1}I_S]. \quad (13)$$

Here the first m entries into the column vector denote the modal voltages in mode k on conductor k to ground. The remaining entries are the amplitudes from conductor $i=m+1, m+2, \cdots, n$ to ground which share the single propagation constant γ_{m+1}.

The physical interpretation of the analysis is of interest and worthy of comment.

Each mode has its own characteristic impedance $[Y][\gamma_k]^{-1}$. This mode characteristic impedance may be interpreted in terms of n simple transmission lines from the conductors to ground and $(n/2)(n-1)$ simple transmission lines that exist between conductors. Thus this modal network consists of separate transmission lines that are coupled by conductor sharing. Since there are m of these networks, a total of $(mn/2)(n+1)$ simple lines are involved in the nondegenerate part of the system. However, since one is talking about a normal mode, only one line voltage can be determined by the boundary conditions in each mode. The degenerate part of the transmission system consists of $(s/2)(s+1)$ simple lines. This system decouples itself from the main system by not exciting or grounding those members that do not share the degeneracy. However, since its eigenvalue is degenerate, s line voltages are determined by the boundary conditions. Thus for a single degeneracy the system reduces to $m+1$ subsystems and a total of $(n/2)(n+1)+[(n-m)/2](n-m+1)$ distinct transmission lines in which exactly n voltages are determined by the boundary conditions. The total system can be terminated by a passive network. This does not depend on the fact that the system is lossless. This reflectionless termination has the ability to transfer energy from one mode to the other to obtain a proper match. In the general case, the modal excitation is a time-dependent quantity governed by the forcing function, the boundary conditions, and the modal characteristic impedances and not by coupling between the modes. This statement is supported readily by expanding (13) in terms of multiple reflections that are useful for transient calculations and by noting that (9) is exactly a lumped-circuit calculation. The implication is and should be that the entire analysis may be based on calculations that occur at the boundary and in which transmission-line concepts are used only in the sense that cause and effect are time delayed and that currents and voltage are related via the characteristic impedance.

References

[1] S. Hayashi, *Surges on Transmission Lines.* Kyoto, Japan: Denki-Shoin, 1955.
[2] E. A. Guillemin, *The Mathematics of Circuit Analysis.* New York: Wiley, 1949.
[3] H. Amemiya, "Time-domain analysis of multiple parallel transmission lines," *RCA Rev.*, vol. 28, pp. 241–276, 1967.
[4] ——, "Matched termination network for multiple parallel transmission lines," *Electron. Lett.*, vol. 3, pp. 13–14, 1967.
[5] H. Hagiwara and S. Okugawa, "Time-domain analysis of multiconductor exponential lines," *Proc. IEEE* (Lett.), vol. 56, pp. 1111–1112, June 1968.

Computation of the Characteristics of Coplanar-Type Strip Lines by the Relaxation Method

TAKESHI HATSUDA

***Abstract*—The characteristics of new strip lines (i.e., a single strip conductor and a two symmetrical strip-conductor coplanar-type strip line, which consist of single- or two-center strip conductors and ground plates on a dielectric substrate and outer ground conductor) are calculated by the relaxation method. The effect of the outer ground conductor on these lines is analyzed, and the characteristic impedance and velocity ratio are determined. The characteristic impedance is determined experimentally, and the maximum values of the discrepancies compared with the calculated values of each of the lines are 2.0–3.0 percent.**

Introduction

Microwave circuits used in a communication satellite, for example, require light weight, small size, and high reliability, so the strip line is suited to these needs. The characteristic impedance and phase-velocity ratio of conventional triplate strip lines are determined by the thickness of the dielectric substrate and its relative dielectric constant, by the width of the strip conductors, and by the height of the line. In order to obtain a smaller line when using the same dielectric substrate and same height of line, or to obtain a more versatile line, different types of new lines must be considered.

The coplanar waveguide (CPW) is very attractive, and it is analyzed in open boundary by using conformal mapping [1]. But closed boundary lines are needed for high-gain amplifier circuits, and lines having side walls can help to miniaturize microwave circuits.

In this short paper, two new types of strip lines [i.e., the single strip-conductor coplanar-type strip line (S-CPS), which has a center strip conductor and ground plates on dielectric substrate as shown in Fig. 1(a), and the two symmetrical strip-conductor coplanar-type strip line (T-CPS), which is shown in Fig. (b)] are analyzed.

Manuscript received June 14, 1971; revised November 29, 1971.
The author is with the Electrical Communication Laboratory, Nippon Telegraph and Telephone Public Corporation, Musasino-si, Tokyo, Japan.

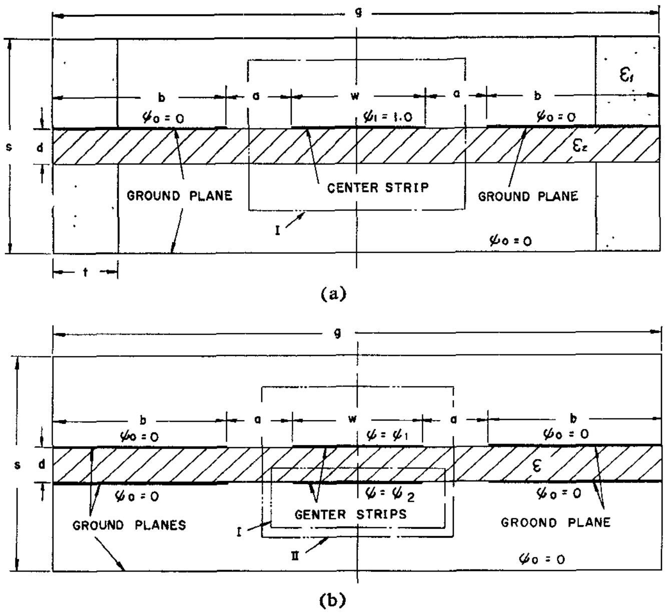

Fig. 1. (a) Single strip-conductor coplanar-type strip line (S-CPS). (b) Two symmetrical strip-conductor coplanar-type strip line (T-CPS).

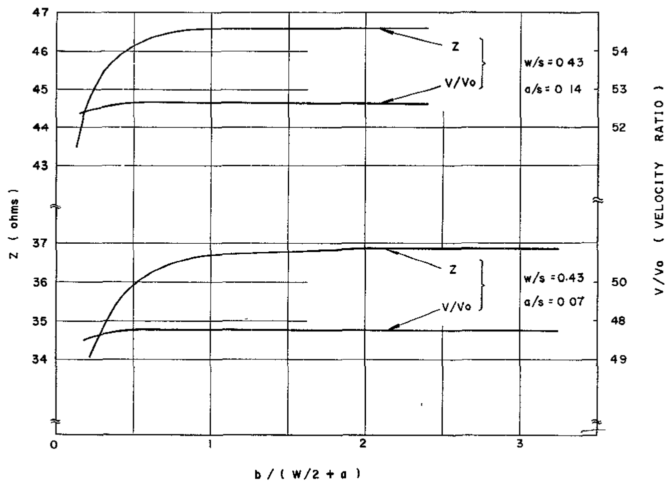

Fig. 2. Z and v/v_0 of S-CPS versus $b/[(w/2)+a]$ ($s=4.3$ mm, $d=0.61$ mm, $\epsilon_2=9.4$, $\epsilon_1=1.0$).

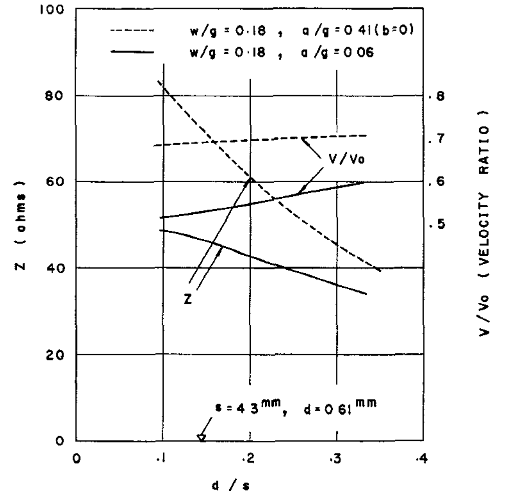

Fig. 3. Z and v/v_0 of S-CPS and conventional type versus d/s.

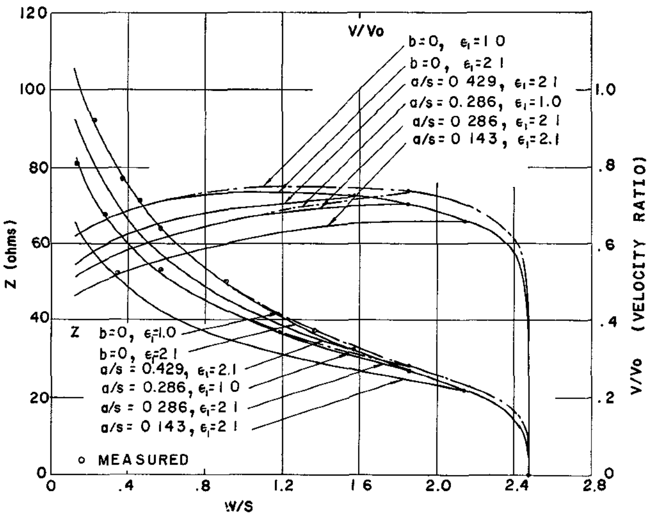

Fig. 4. Z and v/v_0 of S-CPS versus w/s for $b=0$ and $a/s=0.143$, 0.286, 0.429 ($s=4.3$, $g=10.7$, $d=0.61$, $t=1.5$ mm, $\epsilon_2=9.4$).

As shown in Fig. 1(a), the dielectric substrate (whose relative dielectric constant is ϵ_2) is supported by another dielectric (Teflon, whose relative dielectric constant is $\epsilon_1=2.1$), and this is used as a shock absorber and also for maintaining the same potential ($\psi_0=0$) at the ground plate and the outer ground conductor by putting copper foil between the Teflon and the ground plate.

The solution of Laplace's equation for the inhomogeneous case, where the boundaries are comprised of various kinds of dielectrics and multiconductors, is obtained by the use of the relaxation method [2]–[9]. The half area of Fig. 1(a) and the quarter area of Fig. 1(b) are considered for programming.

Characteristics of the S-CPS

The effects of the side wall and the outer ground conductor of the S-CPS are examined first. The characteristics of the S-CPS depend upon the parameter $b/[(w/2)+a]$ as shown in Fig. 2. Values of w/s and a/s used in calculating the characteristics are shown in the figure. From Fig. 2 we see that the characteristic impedance Z and phase-velocity ratio v/v_0 asymptotically approach constant values when the ratio $b/[(w/2)+a]$ is larger than 1.0–1.5. The effect of changes of the s is shown in Fig. 3. The conventional type (i.e., $b=0$) with $w/g=0.18$ is also shown in Fig. 3. We see that the variation of Z is smaller but v/v_0 is larger in the S-CPS than in the conventional type. In the S-CPS, values of Z and v/v_0 tend to become constant when d/s becomes small (i.e., s becomes large).

In Fig. 4, Z and v/v_0 versus w/s of the S-CPS are shown when a/s assumes constant values of 0.143, 0.286, and 0.429. The top solid curve in Fig. 4 shows the characteristics of the conventional type, which has the supporting dielectric (Teflon, $\epsilon_1=2.1$), and the dot and dash curves show the characteristics with no Teflon (i.e., $\epsilon_1=1.0$). The ratios of w/s and v/v_0 for a 50-Ω transmission line of an S-CPS compared with the conventional type of strip line are shown in Table I. The effect of Teflon on the S-CPS is also shown in Fig. 4, and we see that the effect is smaller than for the conventional type.

Characteristics of the T-CPS

Computing programs are made for two modes, i.e., 1) $\psi_1=\psi_2=1.0$ and $\psi_0=0$ for the even mode, and 2) $\psi_1=1.0$, $\psi_2=-1.0$, and $\psi_0=0$ for the odd mode, where ψ_1 and ψ_2 are the potentials of the upper and lower strip conductors, respectively. Four characteristic impedances and four phase-velocity ratios are defined, i.e., Zoe^{I}, Zoe^{II}, $(v/v_0)e^{I}$, and $(v/v_0)e^{II}$ (even-mode case) and Zoo^{I}, Zoo^{II}, $(v/v_0)o^{I}$, and $(v/v_0)o^{II}$ (odd-mode case). Notations I and II indicate the integrating path,

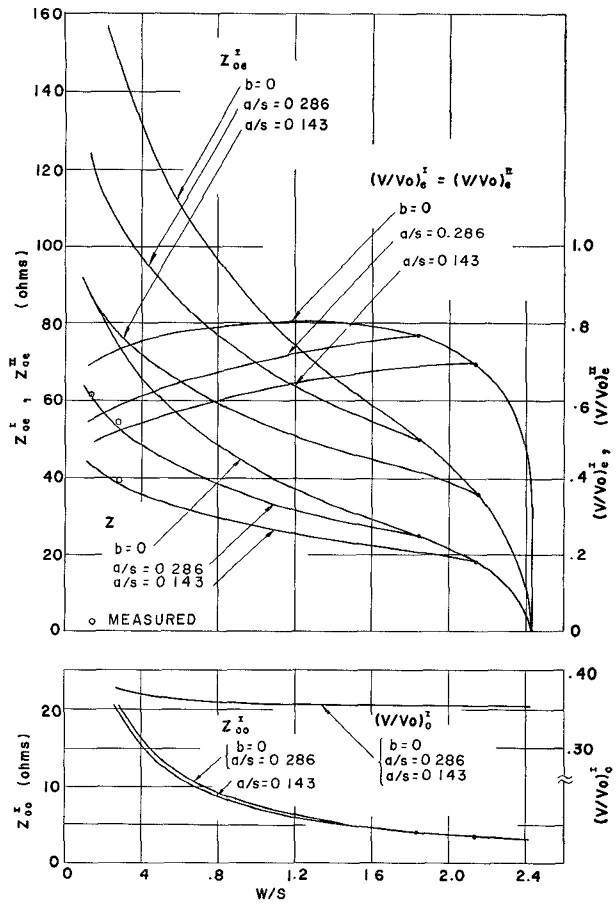

Fig. 5. Z and v/v_0 of T-CPS versus w/s for $b=0$ and $a/s=0.143$, 0.286.

TABLE I

REDUCTION RATIO OF w/s AND v/v_0 OF S-CPS 50-Ω LINE

	w/s	Reduction Ratio (percent)	v/v_0	Reduction Ratio (percent)
Conventional type	0.9		0.73	
$a/s=0.286$	0.64	29	0.62	15
$a/s=0.143$	0.36	60	0.51	30

e denotes even mode, and o denotes odd mode. In the symmetrical strip-conductor case, $Zoe^{II}=Zoe^{I}/2$, $(v/v_0)e^{I}=(v/v_0)e^{II}$, and $Zoo=\infty$.

The effect of the side wall and the outer conductor of the T-CPS shows results similar to the S-CPS case.

The characteristic impedance and phase-velocity ratio versus w/s of the T-CPS when $a/s=0.143$ and 0.286 are shown in Fig. 5. Top curves of Fig. 5 show the characteristics of the conventional-type strip line. Reduction ratios of values of w/s and $(v/v_0)e^{II}$ for a 50-Ω transmission line compared with the T-CPS and conventional type are shown in Table II. From Tables I and II it is apparent that the reduction ratio of w/s and v/v_0 for the T-CPS is larger than for the S-CPS.

Experimental Results

The circular dots plotted in Figs. 4 and 5 are measured points. Experimental strip lines were made from gold-plated Cr–Au thin film. The coaxial to the strip-line connection was achieved by an omni spectra miniature (OSM) adapter. Characteristic impedances Z of the S-CPS and Zoe^{II} of the T-CPS were measured by a time-domain reflectometer. The maximum value of the differences from the calculated values is 2 percent in the conventional type in Fig. 4, and 3 percent in the S-CPS in Fig. 4 and the T-CPS in Fig. 5. This is considered to be due to the uncertainty in the value of the relative dielectric constant of the substrate, equipment construction errors, and measuring errors.

TABLE II

REDUCTION RATIO OF w/s AND $(v/v_0)e^{II}$ OF T-CPS 50-Ω LINE

	w/s	$(v/v_0)e^{II}$
Conventional type	0.75	0.79
$a/s=0.286$	0.36	0.60
Reduction ratio	52 percent	24 percent

TABLE III

ACCURACY OF RELAXATION METHOD COMPARED WITH [10]

		Results of [10]		Results of Relaxation Method and Error				
w/s	g/s	$Zo(\Omega)$	v/v_0	Mesh ($s\times g$)	$Zoe^{II}(\Omega)$	Error (percent)	$(v/v_0)e^{II}$	Error (percent)
0.2	2.0	95.7	0.8965	100×200	94.912	0.82	0.89611	0.044
0.2	2.0	95.7	0.8965	80×160	94.648	1.09	0.89604	0.051
0.2	3.0	97.0	0.9008	100×300	95.780	1.25	0.90081	0.001
0.2	3.0	97.0	0.9008	80×240	95.554	1.49	0.90098	0.019
0.333	2.0	81.2	0.9109	60×120	79.823	1.69	0.90942	0.162
0.333	3.0	81.8	0.9153	60×180	80.785	1.24	0.91566	0.039
0.466	2.0	69.9	0.9209	60×120	69.472	0.61	0.91846	0.178
0.466	3.0	70.9	0.9259	60×180	70.511	0.54	0.92587	0.003

Note: $\epsilon=2.35$, $d/s=0.2$.

Accuracy

The accuracy of results can be checked by comparing with the results of [10], and is shown in Table III where the program T-CPS (even-mode case) is computed by setting $b=0$ (i.e., conventional type). It is seen that the value of the error of Zoe^{II} is 1.49 percent when mesh points of height s are 80 points, $w/s=0.2$, and $g/s=3.0$. The accuracy in regard to $(v/v_0)e^{II}$ is better than Zoe^{II} as shown in Table III. In the calculation of the CPS, as in Figs. 4 and 5, the mesh points of s are 84 points, $g/s=2.48$, and the error becomes small.

Conclusion

By the use of the relaxation method, the characteristics of the S-CPS and the T-CPS are obtained. Merits of the CPS are: 1) The characteristic impedance and phase-velocity ratio become small compared with the conventional-type line due to the existence of ground plates; 2) the CPS is a shielded-type transmission line, so it is suitable to use for high-gain transistor amplifiers or other active circuits; 3) the effect of side wall and other circuits near the center conductor is smaller than conventional type; 4) it is easy to connect shunt elements, for example, in the circuits in transistor amplifiers; 5) it can be used in nonreciprocal magnetic-device applications similar to the CPW and the slot line; and 6) it is easy to use together with the CPS and conventional-type line.

The S-CPS and T-CPS are being used in experimental 4-GHz transistor amplifiers, filters, nonreciprocal magnetic devices, etc. The relaxation method analysis is a quasi-TEM approximation. Thus it has a high-frequency limit, so another analytical method must be considered at high frequencies.

Acknowledgment

The author wishes to thank Dr. R. W. Beatty and Dr. S. Shimada for their helpful comments.

References

[1] C. P. Wen, "Coplanar waveguide: A surface strip transmission line suitable for nonreciprocal gyromagnetic device applications," *IEEE Trans. Microwave Theory Tech. (1969 Symposium Issue)*, vol. MTT-17, pp. 1087–1090, Dec. 1969.

[2] R. V. Southwell, *Relaxation Methods in Theoretical Physics.* New York: Oxford Univ. Press, 1946.

[3] H. E. Green, "The numerical solution of some important transmission-line problems," *IEEE Trans. Microwave Theory Tech.* (*Special Issue on Microwave Filters*), vol. MTT-13, pp. 676–692, Sept. 1965.
[4] M. V. Schneider, "Computation of impedance and attenuation of TEM-lines by finite difference methods," *IEEE Trans. Microwave Theory Tech.*, vol. MTT-13, pp. 793–800, Nov. 1965.
[5] J. W. Duncan, "The accuracy of finite-difference solutions of Laplace's equation," *IEEE Trans. Microwave Theory Tech.*, vol. MTT-15, pp. 575–582, Oct. 1967.
[6] D. H. Sinnot, "The use of interpolation in improving finite difference solutions of TEM mode structures," *IEEE Trans. Microwave Theory Tech.*, vol. MTT-17, pp. 20–28, Jan. 1969.
[7] D. H. Sinnot, G. K. Cambell, C. T. Carson, and H. E. Green, "The finite difference solutions of microwave circuit problems," *IEEE Trans. Microwave Theory Tech.* (*Special Issue on Computer-Oriented Microwave Practices*), vol. MTT-17, pp. 464–478, Aug. 1969.
[8] T. Hatsuda and T. Matsumoto, "Computation of impedance of partially filled and slotted coaxial line," *IEEE Trans. Microwave Theory Tech.* (Corresp.), vol. MTT-15, pp. 643–644, Nov. 1967.
[9] T. Hatsuda *et al.*, "Computation of characteristic impedance of inhomogeneous slotted coaxial lines by relation method," *Electron. Commun. Japan*, vol. 51-B, no. 4, pp. 91–99, Apr. 1968; also (in Japanese), *J. Inst. Elec. Eng.* (*Tokyo*), vol. 51-B, no. 4, pp. 156–163, Apr. 1968.
[10] D. L. Gish and D. Graham, "Characteristic impedance and phase velocity of a dielectric-supported air strip transmission line with side wall," *IEEE Trans. Microwave Theory Tech.*, vol. MTT-18, pp. 131–148, Mar. 1970.

Solutions for Some Waveguide Discontinuities by the Method of Moments

VU KHAC THONG

***Abstract*—The electromagnetic boundary value problem of two waveguides coupled by an aperture or an aperture in a waveguide radiating into free space may be described by an integral equation. An analytical solution to this integral equation cannot be readily found due to the complexity of the kernel. However, extremely useful results may be obtained if the method of moments is employed to reduce the integral equation to a matrix equation which can be solved by known methods. In this short paper, series and shunt slots in a rectangular waveguide are analyzed using this technique.**

The electromagnetic boundary value problem of two waveguides coupled by an aperture or an aperture in a waveguide radiating into free space may be considered to be solved if the tangential components of the electric field at the aperture are determined for various excitation conditions. For a system of two waveguides coupled by an aperture S, the integral equation for the tangential components of the electric field at the aperture can be shown to be [1]

$$n \times H^{inc} = j\omega\epsilon n \times \int_s [\bar{G}_h^{(1)}(r \mid r_0) + \bar{G}_h^{(2)}(r \mid r_0)] \cdot [n \times E(r_0)]\, ds_0. \quad (1)$$

$\bar{G}_h^{(1)}$, $\bar{G}_h^{(2)}$ are the magnetic Green's dyadics for the separate waveguides satisfying equations such as

$$\nabla \times \nabla \times \bar{G}_h^{(1)}(r \mid r_0) - k^2\bar{G}_h^{(1)}(r \mid r_0) = -\bar{I}\delta(r - r_0)$$
$$n \times \nabla \times \bar{G}_h^{(1)}(r \mid r_0) = 0$$

at the guide walls. H^{inc} is the magnetic field of the exciting mode. It is assumed that the waveguides are connected to matched loads.

Analytical solution to the integral equation (1) may not be readily found due to the complexity of the kernel. However, extremely useful approximate results may be obtained if it is noted that (1) has the form

$$Lf = (L^{(1)} + L^{(2)})f = g \quad (2)$$

where L, $L^{(1)}$, $L^{(2)}$ are linear operators. By the method of moments [2] (2) can be reduced to an Nth-order matrix equation. If the basis func-

Manuscript received June 14, 1971; revised November 29, 1971.
The author is with the Department of Electrical Engineering, Monash University, Clayton, Victoria 3168, Australia.

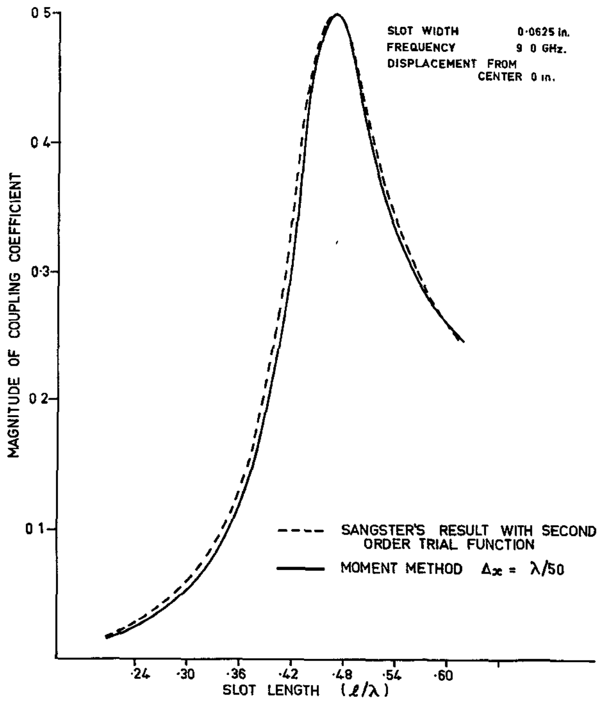

Fig. 1. Magnitude of coupling coefficient as a function of slot length for a series slot in the broadwall coupling two rectangular waveguides.

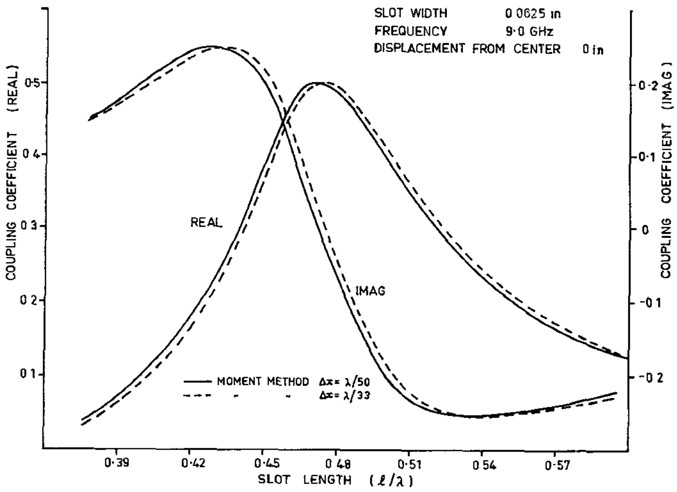

Fig. 2. Coupling coefficient as a function of slot length for a series slot in the broadwall coupling two rectangular waveguides.

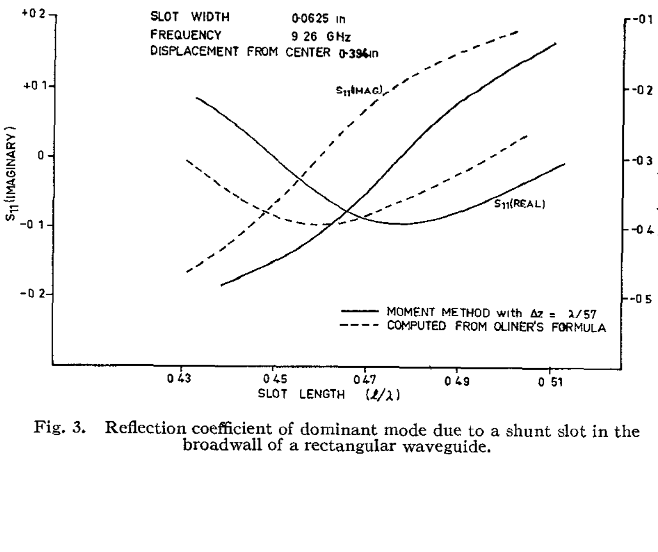

Fig. 3. Reflection coefficient of dominant mode due to a shunt slot in the broadwall of a rectangular waveguide.